



Unsymmetric cyanines: chemical rigidization and photophysical properties

Martin Sczapan^a, Wolfgang Rettig^{a,*}, Yulia L. Bricks^b,
Yuri L. Slominski^b, Alexei I. Tolmachev^b

^aHumboldt-Universität zu Berlin, W.-Nernst-Institut für Physikalische und Theoretische Chemie, Bunsenstr.1, 10117 Berlin, Germany

^bInstitute for Organic Chemistry of the National Academy of Science of Ukraine, Kiev, Ukraine

Received 22 February 1999; accepted 22 February 1999

Abstract

Cyanines with unsymmetric donor groups are investigated by steady state and time-resolved fluorescence measurements. Several chemically rigidized derivatives are compared, and their synthesis is described. In several cases, rigidization leads to an increase of the nonradiative decay rate constants. This unusual behaviour is explained within a model of multiple emissive states. © 1999 Elsevier Science S.A. All rights reserved.

Keywords: Unsymmetric cyanines; Chemical rigidization; Photophysical properties; Time-resolved fluorescence; Conical intersections

1. Introduction

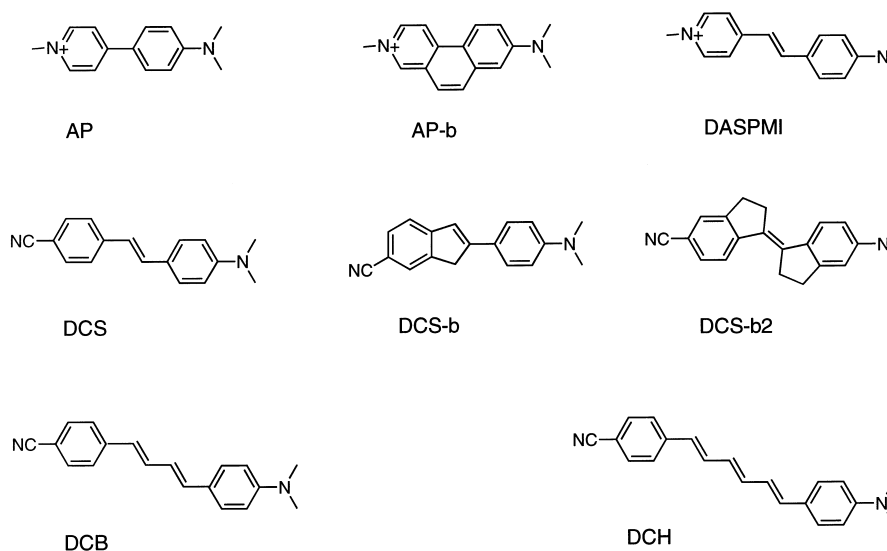
Cyanine dyes are widely used for application due to their versatile properties. Their absorption range can readily be predicted [1–5], they show fluorescence properties which render them useful e.g. as laser dyes [6], as mode-locking dyes and as fluorescence probes in molecular biology [7,8], and they possess promising nonlinear-optical properties [9,10]. The fluorescence properties are strongly influenced by the photochemical processes which compete with the fluorescence process. The most-discussed photochemical pathways incorporate twisting around one of the bonds, intermediate in bond order between single bond and double bond. The classical photochemical mechanism involves a twisted excited intermediate P^* which decays nonradiatively to the ground state leading to either the *cis*- (or *trans*-) isomer and the starting material E [11]. Most cyanine dyes possess several different flexible bonds, and the isomerization around them leads to different product isomers. It is one of the key questions, which of the bonds is the most reactive one leading preferentially to isomerization. A step in this direction has been attempted by theoretical models and calculations [6,12–17]. A different approach is to test a series of cyanines with selectively bridged bonds and to compare their fluorescence behaviour [6,18–20]. If the bridging excludes the access to the perpendicular minimum

P^* then this photochemical transition does not contribute to the observed fluorescence quenching, and therefore the observation of increased fluorescence quantum yields for certain bridged analogs helps to identify the most reactive bonds. This approach has been most fruitful in the concept of twisted intramolecular charge transfer (TICT) states, which refer to the twisting of single bonds in merocyanine-type systems. This model allows a prediction of the bridging substitution pattern, and many examples of bridged and unbridged compound pairs are known (for reviews see [21–24]).

Recently, some unsymmetric cyanine dyes have also been shown to emit from several excited species (multiple fluorescence). One example is the anilino-pyridinium system AP [25], another one DASPMI (and derivatives) [26–29]. In both cases, bridged model compounds such as AP-b (see Scheme 1) positively identified the twisting motion as the reactive coordinate, and time-resolved studies established the precursor–successor relationship of the fluorescence contributions [26,27].

Interestingly, bridging a certain bond in a polymethinic or polyenic molecule does not always lead to enhancement of the fluorescence quantum yield, as would be expected from the loose bolt theory [30,31]. Anti-loose-bolt behaviour, i.e. a reduced fluorescence quantum yield for some of the bridged derivatives, has been observed in donor–acceptor stilbenes such as DCS-b2 as compared to DCS [32]. On the other hand, if different bonds are bridged, as in DCS-b, an

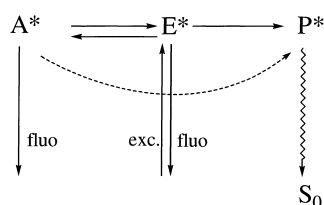
*Corresponding author.



Scheme 1. Structures of unbridged and bridged dye systems in the polyene series.

increase of the quantum yield is observed [32]. This can be understood as a direct indication of the involvement of excited-state conformations with twisted single bonds. The series of polyenes DCS, DCB and DCH, is in fact connected with multiple fluorescence [33,34].

It is well-known that the isomerization of ethylene, polyenes and probably also cyanines proceeds through a conical intersection (CI) or “photochemical funnel” [35,36] which can therefore be identified with P^* , and recent high-level quantum-chemical calculations could even elucidate the structure of this conical intersection [37] pointing to the importance of more than one bond being involved in the twisting process. Thus, butadiene CI involves three perpendicularly twisted bonds and four unpaired electrons [37]. In view of the vast evidence that single-bond twisting can lead to dual fluorescence [22,23], the possibility arises to combine the seemingly separate observations of multiple fluorescence, anti-loose bolt behaviour and photochemical isomerization through photochemical funnels into a common mechanistic model involving fluorescent and nonfluorescent twisted product species in the excited state. An early mechanistic scheme has been introduced a decade ago with the three-state model (Scheme 2) to explain the fluorescence



Scheme 2. Three-state kinetic model used to explain the fluorescence behaviour of donor-acceptor polyenes [38,39]. E^* is the highly emissive planar conformation, A^* corresponds to a single-bond twisted polar species, and P^* to the photochemical funnel leading nonradiatively to the ground state.

behaviour of DCS [38]. In the present study, we apply this model to explain the anti-loose bolt behaviour of a series of unsymmetric cyanine dyes *s3-s* and derivatives (see Scheme 6).

2. Experimental

2.1. Synthesis

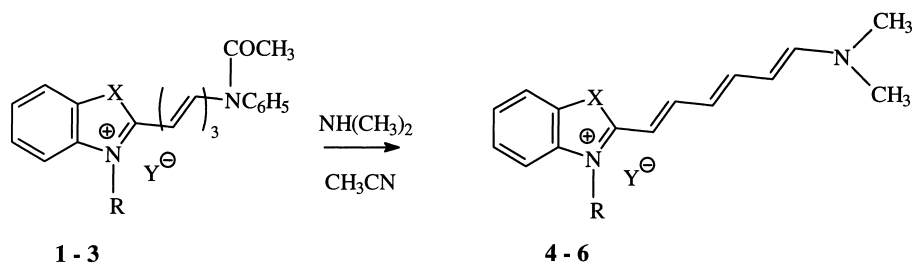
Hexamethinehemicyanines **4–6** containing the dimethyl-amino group as an electron-donor fragment have been synthesized by the condensation of N-containing heterocyclic acetanilidohexatrienyl derivatives **1–3** [40] with the corresponding amine in acetonitrile or iso-propanol (Scheme 3).

A number of hexamethinehemicyanines containing bridge groups in the polymethine chain have been obtained. By the condensation of ethyl *p*-toluenesulphonates 2-methyl-benzoxazole- or benzothiazole **7–8** with 1,4,5,8-tetrahydro-2,7-dimethoxynaphthalene **9** under the conditions described previously [41,42], salts **10–11** have been prepared. These contain the methoxy group which can be substituted by various nucleophilic moieties [41], for example by the dimethylamino group (see Scheme 4).

The synthesis of hexamethinehemicyanines containing a neopentylene bridge group in the β,δ -positions of the chromophore was started from the benzothiazole acetanilidohexatrienyl derivative **14** [43]. Condensation of this compound with dimethylamine resulted in product **15** (Scheme 5).

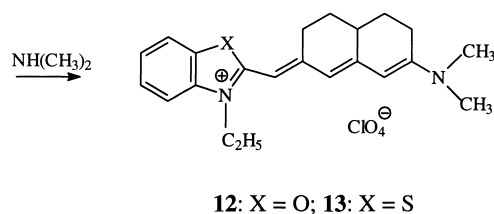
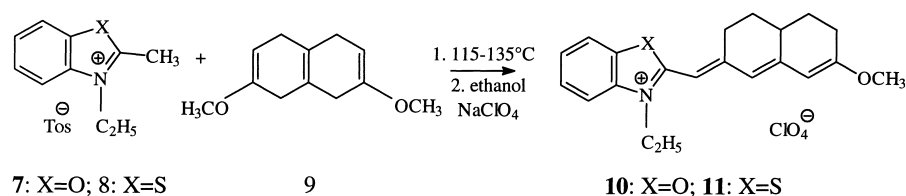
All chemicals for the synthesis were purchased from Merck.

The chemical structures of the synthesized compounds were confirmed by $^1\text{H-NMR}$, $^{13}\text{C-NMR}$ and elemental analysis and their purity was checked by reversed phase HPLC (HPLC setup from Merck-Hitachi; RP18 column;



- 1:** X = C(CH₃)₂, R = CH₃, Y = BF₄;
2: X = O, R = C₂H₅, Y = ClO₄;
3: X = S, R = C₂H₅, Y = I;
4: X = C(CH₃)₂, R = CH₃, Y = BF₄;
5: X = O, R = C₂H₅, Y = ClO₄;
6: X = S, R = C₂H₅, Y = I;

Scheme 3. Synthetic scheme for the unbridged cyanine dyes.

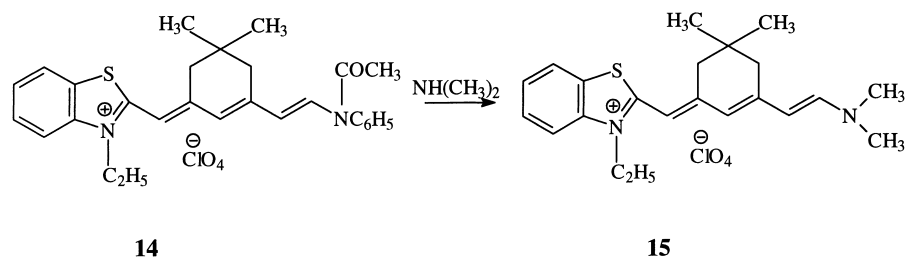


Scheme 4. Synthetic scheme for bridging pattern in cyanines.

CH₃CN+H₂O:75+25 as eluent). The NMR spectra were obtained with a 500 MHz NMR spectrometer Varian Unity_{plus}500. The melting points (m.p.) measured with a digital melting point analyser IA 9100 (Kleinfeld GmbH) are uncorrected.

2-(6-Dimethylaminohexa-1,3,5-trien-1-yl)-1,3,3-trimethyl-3H-2-indolium tetrafluoroborate (**4**). 30% Aqueous solution of dimethylamine (0.2 g) was added to acetanili-

dohexatrienyl substituted 1,3,3-trimethyl-indolium tetrafluoroborate (**1**) (0.46 g 0.001 mol) suspended in isopropanol (5 ml). The mixture was refluxed for 1 min (until the precipitate was dissolved completely). After cooling, it was allowed to stand for 2 h at 4°C. Then the precipitate was filtered off and washed with isopropanol and ether. Yield 0.34 g. The product was recrystallized from acetic acid.



Scheme 5. Synthetic scheme for alternative bridging pattern in cyanines.

Hexamethinecyanines **5–6** have been obtained under analogous conditions.

2-[(7-Methoxy-4,4a,5,6-tetrahydro-2(3H)naphthaldehyde)methyl]-3-ethyl benzoxazolium perchlorate (**10**). 2-Methyl-3-ethylbenzoxazolium *p*-toluenesulphonate **7** (1.6 g, 0.0054 mol) and 2,7-dimethoxy-1,4,5,8-tetrahydronaphthalene **9** (1.4 g, 0.007 mol) were fused together at 115–117°C for 15 min. The fusion was treated with dry ether (twice 10 ml) and dissolved in ethanol. The product was precipitated with the aqueous solution of sodium perchlorate (yield 2.0 g) and crystallized from isopropanol. Yield 1.3 g (61%), m.p. 210–212°C, λ_{\max} 467 nm, ϵ 4.08×10^4 l/mol cm (in methanol). Found, %: C, 59.70; H, 5.78; N, 3.41. Calculated, % for $C_{21}H_{24}ClN_2O_6$: C, 59.78; H, 5.73; N, 3.32.

Compound **11** has been obtained in an analogous way [41].

2-[(7-Dimethylamino-4,4a,5,6-tetrahydro-2(3H)naphthaliden)-methyl]-3-ethylbenzoxazolium perchlorate (**12**). Compound **10** (0.6 g, 0.0015 mol) and 30% aqueous dimethylamine (3 ml) were refluxed for 2 min. After cooling, the dye was filtered off, washed with ethanol (twice 2 ml) and ether (yield 0.32 g). The product was recrystallized from methanol. Yield 0.16 g (24%), m.p. 221–222°C, λ_{\max} 553 nm, ϵ 19.02×10^4 l/mol cm (in methanol). Found, %: C, 60.92; H, 6.30; N, 6.39. Calculated, % for $C_{22}H_{27}ClN_2O_5$: C, 60.75; H, 6.26; N, 6.44.

Hemicyanine **13** was obtained similarly.

2-[6-Dimethylamino-2,4-(β,β -dimethyltrimethylene)-hexa-1,3,5-trien-1-yl]-3-ethylbenzothiazolium perchlorate (**15**). The suspension of acetanilidohexatrienyl substituted benzothiazolium perchlorate **14** (0.001 mol) was heated in absolute ethanol (5 ml) to boiling and then 30% aqueous dimethylamine (0.2 g) was added. The mixture was refluxed for 2 min and the resulting precipitate was filtered off 2 h later.

In order to facilitate reading the paper, the compounds have been abbreviated with letters and suffixes which contain the various variations of the bridging structure and of the different heteroatoms present. The structures of the compounds investigated, and their abbreviations are given in

Scheme 6. The dye characteristics including synthetic and analytical information are presented in Table 1.

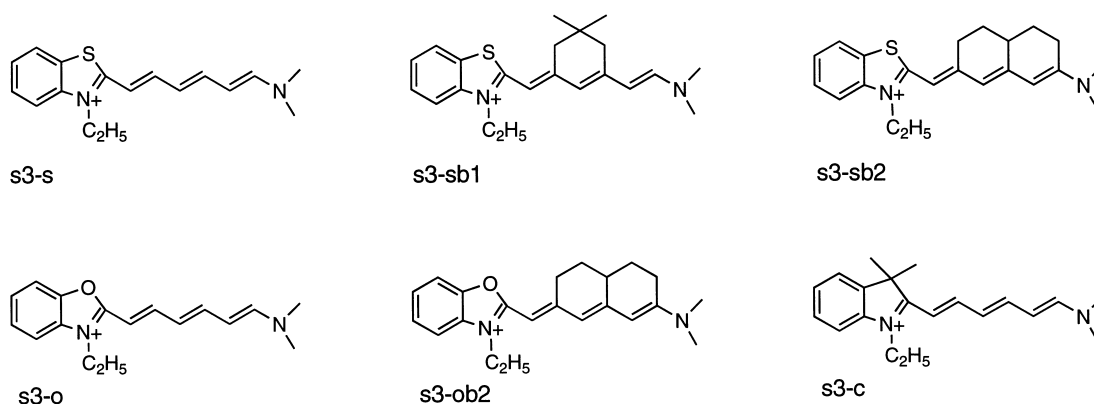
2.2. Spectroscopy

Spectroscopic grade ethanol (Merck Uvasol) was used as solvent for all measurements. The solutions were prepared to optical densities of 0.1–0.15 for steady state and 0.15–0.25 for time resolved spectroscopy, respectively. Absorption spectra were measured on an AT UNICAM UV4 UV–Vis spectrometer and corrected fluorescence spectra on an SLM AMINCO AB2 spectrometer. Fluorescence quantum yields were determined with Rhodamin 101 in ethanolic solution as a standard ($\phi_f=1$). Fluorescence decay curves were recorded with the time-correlated single photon counting technique using an equipment described in detail elsewhere [44]. Synchrotron radiation from the Berlin electron storage ring BESSY operating in the single bunch mode was used for excitation [44]. The decay times were fitted using the iterative reconvolution procedure (Marquard algorithm), which allowed a time resolution down to 0.1 ns and a relative precision of about 0.1 ns. For measurements at low temperatures, a home-made liquid nitrogen cooled cryostat was used.

3. Results

Absorption and fluorescence spectra do not change upon prolonged illumination at room temperature in ethanol. This seems to indicate the absence of a net photoisomerization possibly due to the short ground state lifetime of any photoisomers formed which quickly react back to the all-*trans* isomer in a thermally controlled reaction.

Figs. 1 and 2 show the spectral results for the example of an unbridged and a bridged cyanine derivative. The fluorescence intensity increases strongly with decreasing temperature, but the effect is clearly larger for the bridged derivative s3-sb1, i.e. it has a sizeably lower fluorescence quantum yield at room temperature. This can also be seen in



Scheme 6. Structures of the investigated unbridged and bridged cyanine compounds and their abbreviation used in the text of the paper.

Table 1
Characteristics of the hexamethinehemicyanines synthesized

No.	Yield (%)	m.p. (°C)	λ_{\max} (nm) ($\epsilon \times 10^{-4}$ l/mol cm)	Found (%)	Empirical formula	Calculated (%)	NMR δ (ppm ^c)
4=s3-c	59	206–207 ^a	571 (16.99) (methanol)	F 20.60, 20.72 N 7.52, 7.40	C ₁₉ H ₂₅ BF ₄ N ₂	F 20.54 N 7.60	¹ H: 1.637 (s, 6H), 3.206 (s, 3H), 3.433–3.458 (d, $J=12.5$ Hz, 6H), 5.777–5.803 (d, $J=13.1$ Hz, 1H), 6.322–6.372 (t, $J=12.6$ Hz, 1H), 6.940–6.956 (d, $J=7.9$ Hz, 1H), 7.118–7.148 (d, $J=7.4$ Hz, 1H), 7.280–7.326 (m, 2H), 7.728–7.780 (t, $J=13.1$ Hz, 1H), 7.789–7.842 (t, $J=13.1$ Hz, 1H), 7.976–7.998 (d, $J=11.3$ Hz, 1H) ¹³ C: 28.100, 38.824, 47.115, 48.448, 99.906, 108.320, 109.038, 122.133, 122.461, 123.867, 128.398, 140.333, 143.105, 152.816, 162.866, 164.287, 170.950
5=s3-o	32	173–174 ^b	544 (21.14) (methanol)	Cl 9.27; 9.39	C ₁₇ H ₂₁ ClN ₂ O ₅	Cl 9.61	¹ H: 1.470–1.499 (t, $J=7.2$ Hz, 3H), 1.568 (s, 6H), 4.148–4.163 (q, unresolved, 2H), 5.723 (broad, 2H), 6.367 (broad, 1H), 7.253–7.830 (m., 7H) ¹³ C: 13.085, 18.454, 35.145, 39.531, 46.445, 58.495, 86.661, 105.166, 109.895, 111.075, 119.541, 125.172, 125.981, 147.043, 153.185, 160.813
6=s3-s	37	208–209 ^b	580 (19.58) (methanol)	I 30.79, 30.84	C ₁₇ H ₂₁ IN ₂ S	I 30.37	¹ H: 1.451–1.479 (t, $J=7.1$ Hz, 3H), 3.118 (s, 3H), 3.433 (s, 3H), 4.292–4.306 (q, unresolved, 2H), 5.812 (t, unresolved, 1H), 6.259 (d, unresolved, 1H), 6.432 (t, unresolved, 1H), 7.311–8.065 (m, 7H) ¹³ C: 12.812, 34.754, 41.983, 112.059, 122.742, 125.042, 127.919, 160.842
12=s3-ob2	24	221–222 ^b	553 (19.02) (methanol)	C 60.92, 60.97 H 6.30, 6.21 N 6.39, 6.25 C 58.92, 58.95	C ₂₂ H ₂₇ ClN ₂ O ₅	C 60.75 H 6.26 N 6.44 C 58.59	¹ H: 1.276–1.305 (t, $J=7.3$ Hz, 3H), 1.382–1.433 (m, 2H), 2.001–2.012 (m, 2H), 2.419–3.014 (m, 5H), 3.249 (s, broad 6H), 4.120–4.163 (q, $J=6.9$ Hz, 2H), 5.438 (s, 1H), 5.903 (s, 1H), 6.551 (s, 1H), 7.216–7.289 (t, $J=7.5$ Hz, 1H), 7.364–7.393 (t, $J=7.0$ Hz, 1H), 7.605–7.622 (d, $J=8.3$ Hz, 1H) ¹³ C: 12.322, 27.550, 28.371, 28.749, 34.251, 38.330, 40.962, 82.566, 102.571, 103.455, 109.923, 110.340, 123.577, 125.519, 130.530, 146.404, 158.665, 160.204, 167.002, 167.623
13=s3-sb2	24	229–231 ^b	582 (18.77) (methanol)	H 6.07, 6.20 Cl 7.80, 7.86 C 58.14, 58.09	C ₂₂ H ₂₇ ClN ₂ O ₄ S	H 6.03 Cl 7.86 C 58.33	¹ H: 1.241–1.283 (t, $J=6.8$ Hz, 3H), 1.391–1.433 (m, 2H), 1.996–2.038 (m, 2H), 2.494–2.900 (m, 5H), 3.263–3.332 (d, 6H), 4.279–4.302 (q, unresolved, 2H), 5.992 (s, 1H), 6.070 (s, 1H), 6.382 (s, 1H), 7.249–7.298 (t, $J=7.4$ Hz, 1H), 7.462–7.513 (t, $J=7.0$ Hz, 1H), 7.557–7.583 (d, $J=8.0$ Hz, 1H), 7.844–7.870 (d, $J=7.8$ Hz, 1H) ¹³ C: 11.894, 27.610, 28.221, 28.752, 30.810, 34.122, 41.164, 96.866, 111.931, 122.478, 123.556, 125.849, 139.738, 154.884, 158.156, 166.645, 168.261
15=s3-sb1	59	195–197 ^b	591 (18.0) (acetonitrile)	H 6.51, 6.59 N 5.87, 5.78	C ₂₂ H ₂₉ ClN ₂ O ₄ S	H 6.45 N 6.18	¹ H: 1.035 (s, 6H), 1.279–1.307 (t, $J=7.2$ Hz, 3H), 2.492 (s, 2H), 2.580 (s, 2H), 3.312 (s, 6H), 4.355–4.398 (q, $J=7.3$ Hz, 2H), 5.809–5.832 and 8.026–8.050 (2xd, $J=11.8$ Hz, 2H), 6.245 (s, 1H), 6.541 (s, 1H), 7.339–7.371 (m, 1H), 7.536–7.569 (m, 1H), 7.676–7.692 (d, $J=8.3$ Hz, 1H), 7.955–7.970 (d, $J=7.3$ Hz) ¹³ C: 12.128, 27.861, 31.575, 37.917, 40.879, 44.229, 45.817, 98.842, 105.043, 112.584, 122.732, 124.208, 125.514, 128.093, 139.640, 155.363, 157.043, 158.135, 163, 690

^a Crystallized from acetic acid.

^b Crystallized from methanol.

^c NMR spectra for compounds 4, 5, 6 have been measured in CDCl₃ and for compounds 12, 13, 15 – in DMSO-d₆.

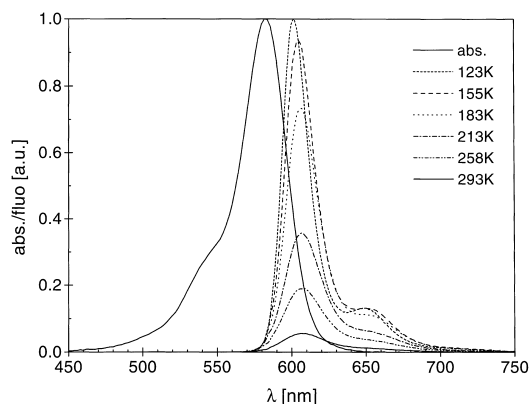


Fig. 1. Absorption spectrum of s3-s in ethanol at 293 K, and fluorescence spectra at various temperatures.

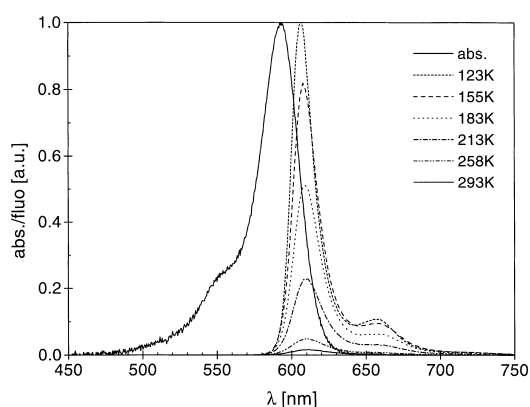


Fig. 2. Absorption spectrum of s3-sb1 in ethanol at 293 K, and fluorescence spectra at various temperatures.

Table 2 which summarizes all spectral and photophysical results.

Generally, the spectra of the unbridged compounds are broadened with respect to those of the bridged ones. In both cases, this broadening reduces continuously for lower temperatures. Likewise, the fluorescence maxima show some blue shift with decreasing temperature. This blue shift is

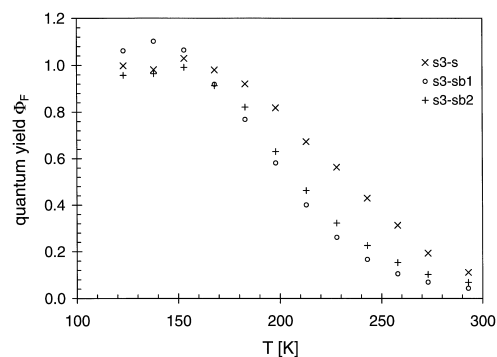


Fig. 3. Fluorescence quantum yields of s3-s and bridged derivatives as a function of temperature.

stronger for the unbridged compounds than for the bridged ones. Some comparative results are listed in Table 2. Generally, the fluorescence spectra are somewhat narrower than the absorption spectra. If the broadening of the spectra is understood as deriving from the population of thermally available conformers, then these results can be taken as evidence that some of these conformers are nonemissive (reduction of the fluorescence width) and that the bridged compounds populate a reduced conformational manifold.

The lifetimes measured at room and lower temperatures were all strictly monoexponential. In the multiple conformer model, these species should therefore be kinetically equilibrated on the excited-state potential energy surface. The broader fluorescence spectra for the unbridged compounds therefore indicate that several equilibrated excited species are emitting and that this number is reduced for the bridged compounds and upon lowering the temperature.

Figs. 3 and 4 display the temperature dependence of the fluorescence quantum yields. At intermediate temperatures, the lowered quantum yield for the bridged s3-s derivatives is especially sizeable. At temperatures below 150 K, quantum yields of 1 are reached.

For s3-o and its bridged derivative s3-ob2, the effect is opposite, i.e. the bridged compound possesses slightly larger

Table 2
Spectroscopic and photophysical parameters of the cyanine dyes investigated in ethanol

		s3-s	s3-sb1	s3-sb2	s3-o	s3-ob2	s3-c
max Abs.	nm	583.5	593.5	585	547	556	571
max Fluo. (293 K)	nm	607	610	600	572	568	603
max Fluo. (123 K)	nm	601	607	598	566	568	590
Stokes-Shift	cm ⁻¹	663	456	427	799	380	929
FWHM (293 K)	cm ⁻¹	950	760	740	1050	730	1100
FWHM (123 K)	cm ⁻¹	570	460	470	630	470	660
φ _F	at 293 K	0.094	0.034	0.045	0.098	0.145	0.067
φ _F	at 228 K	0.563	0.261	0.322	0.531	0.610	0.508
τ _{max}	ns (T<150 K)	2.76	2.60	2.83	2.19	2.33	2.05
k _{fluo}	10 ⁸ s ⁻¹	3.62	3.85	3.53	4.57	4.29	4.88
k _{nr} (293 K)	10 ⁹ s ⁻¹	2.5	8.1	5.0	2.3	1.9	3.3
k _{nr} (228 K)	10 ⁹ s ⁻¹	0.31	1.05	0.72	0.26	0.22	0.33
Arrh.-Plot ln(A/s)		29±2	30±2	29±2	30±2	29±2	30±2
Arrh.-Plot E _A	kJ/mol	18±3	17±3	17±3	19±3	18±3	20±3

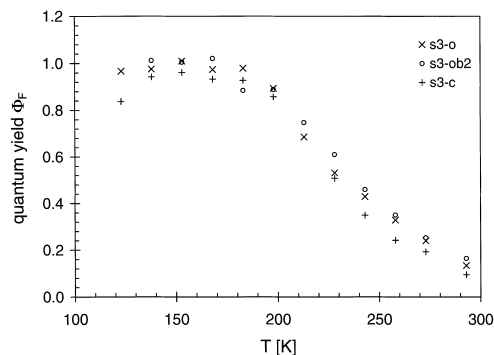


Fig. 4. Fluorescence quantum yields of s3-o, s3-c and a bridged derivative as a function of temperature.

fluorescence quantum yields. The carbon-derivative s3-c shows a very similar temperature dependence as s3-o.

The values for k_{nr} were estimated from the fluorescence lifetime at temperature T ($\tau(T)$) and the limiting fluorescence lifetime τ_{max} reached at low temperature using the following equation:

$$k_{nr}(T) = \frac{1}{\tau(T)} - \frac{1}{\tau_{max}} \quad (1)$$

The results were confirmed by the values for k_{nr} obtained from temperature-dependent fluorescence quantum yield ($\Phi_F(T)$) measurements (Eq. (2)):

$$k_{nr}(T) = \frac{1}{\tau_{max}} \cdot \left(\frac{1}{\Phi_F(T)} - 1 \right) \quad (2)$$

The Arrhenius plots for sulfur and oxygen containing cyanines are displayed in Figs. 5 and 6. At all temperatures, k_{nr} for the two bridged sulfur compounds is sizeably faster than for the unbridged s3-s, but the contrary holds for the oxygen-containing pair where k_{nr} for s3-ob2 is slightly slower than for the case of s3-o.

The Arrhenius parameters are summarized in Table 2. All Arrhenius slopes are roughly equal (16–18 kJ/mol) and close to or smaller than the mean activation energy of solvent viscosity (20 kJ/mol for ethanol in the low-temperature range investigated here [44]).

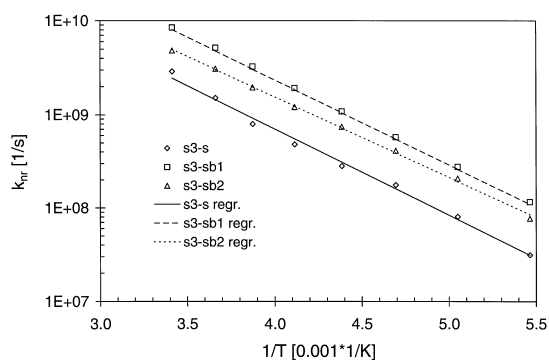


Fig. 5. Arrhenius plot for the nonradiative decay rate constant of s3-s and its two bridged derivatives.

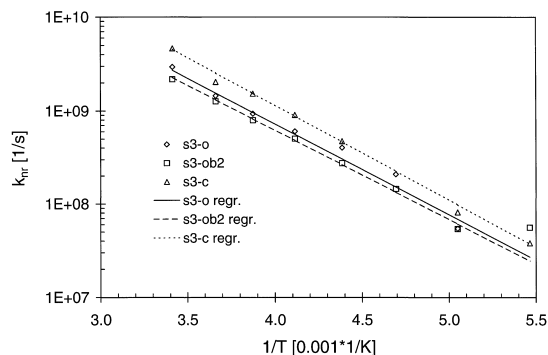


Fig. 6. Arrhenius plot for the nonradiative decay rate constant of s3-o, s3-c and one bridged derivative.

4. Discussion

There are four key observations which are unusual in the photophysics of the bridged and unbridged cyanines and which find their simple explanation in the light of the multiple-state model:

1. The fluorescence spectra of the bridged compounds are narrower than those of the unbridged compounds.
2. The spectra show a small but significant blue shift upon cooling which is most prominent for the unbridged compounds.
3. For the benzthiazolium compounds (s3-s and derivatives), bridging reduces the fluorescence quantum yields and enhances the nonradiative rate constant k_{nr} , while for the benzoxazolium compounds (s3-o), the fluorescence quantum yield is slightly larger than for the bridged compound. The behaviour of s3-s is very unusual in the sense, that for most dyes rigidization leads to increased quantum yields whereas here the contrary is observed. In terms of the loose bolt theory [30,31], the behaviour of s3-o is the normal one, whereas that of s3-s can be termed an “inverse loose-bolt behaviour”.
4. The Arrhenius slopes for all the compounds are nearly equal and correspond to or are slightly lower than the activation energy of solvent viscosity.

We will discuss these points in the context of the multiple-state model in order to emerge with a coherent picture of the photophysical processes involved.

4.1. Multiple fluorescence contributions

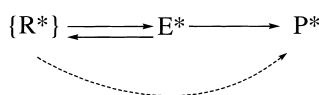
The broadened spectra and their narrowing upon sufficient cooling can be understood by assuming an equilibrium of various fluorescent conformers slightly differing in their emission energies and involving a large-amplitude relaxation for their interconversion. Given that at room temperature and also at low temperatures but not too high solvent viscosity, this interconversion process can be expected to be faster than the time resolution of our equipment (0.1 ns), it is understandable that we observe only single exponential

fluorescence decay behaviour. But the various spectral contributions broaden somewhat the observed spectra, and in a general sense, this broadening is expected to increase with the number of emitting conformers present. The narrowed spectra for the bridged compounds therefore indicate a reduced number of emitting conformers which suggests that the large-amplitude relaxation process is linked with bond twisting. At sufficiently low temperature, solvent viscosity is high enough to stop one or all of these relaxation paths, and only the primary excited slightly blue shifted conformer remains and leads to the narrowed and blue shifted spectra at low temperature. These effects are most prominent, as expected, for the unsubstituted compounds which possess the largest number of flexible bonds and therefore possible conformers.

We can summarize this behaviour in a multiple state model (Scheme 7) which is strongly reminiscent of the three-state model introduced for the stilbenes (Scheme 2). We summarize all the possible relaxed species which are in excited-state conformational equilibrium with the primary excited E^* species by a common label R^* . Part of the conformational manifold of R^* can be reduced or totally suppressed by selective bond bridging. The relaxation channel to R^* occurs in addition to a further channel leading to species P^* which corresponds to the “phantom singlet” state in stilbene and leads nonradiatively to the ground state, i.e. is the main source of viscosity-dependent fluorescence quenching. It is generally believed that the P^* formation process probably involves several twisted bonds and corresponds to a conical intersection with the ground state. This has been investigated recently by theoretical calculations, both for butadiene and protonated Schiff bases [37,45,46] which resemble in their electronic structure to the asymmetric cyanines studied here and which are model compounds for the primary visual process.

4.2. Inverse loose bolt effect

The different behaviour upon bridging of s3-s and s3-o with respect to the nonradiative decay can then be understood on the basis of different intrinsic fluorescence properties of R^* and on the population efficiency of R^* . If the intrinsic nonradiative decay channel of R^* is unimportant, then its efficient population should lead to an increase of the fluorescence quantum yield and a corresponding decrease of the nonradiative decay rate constant, with respect to the hypothetical situation where only E^* and the quenching state P^* are available. Of course, the situation is complicated by



Scheme 7. Multiple state model as an extension of the three-state kinetic model of Scheme 2. Several different relaxed conformations $\{R^*\}$ are in thermal equilibrium and depopulate nonradiatively via the conical intersection P^* .

the fact that P^* probably involves the twisting of several bonds, and therefore, the comparison of bridged and unbridged compounds changes several factors at once, possibly also the detailed geometry of the active conical intersection. Nevertheless, this zero-order model allows to explain in a simple manner the unusual behaviour of the inverse loose bolt effect for s3-s, as well as for donor–acceptor stilbenes [32,39].

In the case of s3-o, where a slight but normal loose bolt effect is observed, i.e. where the fluorescence quantum yields increase with twisting of flexible bonds, two possibilities can be used to explain this behaviour:

1. either the population of R^* is ineffective, e.g. because R^* is energetically slightly above E^* ;
2. or the intrinsic nonradiative decay of R^* through $k_{nr}(R^*)$ is stronger than the decay of E^* through $k_{nr}(P^*)$.

Which of these two possibilities is more likely can be judged by inspection of the spectra. The halfwidths of the bridged compounds are very similar and significantly smaller than the halfwidths of the unbridged compounds. This difference also holds for low temperatures (see Table 2). If this spectral broadening is taken as an evidence for emission from multiple conformers R^* , then we can conclude that population of R^* occurs in both cases s3-s and s3-o and that explanation (2) is more appropriate.

In any case, from the fact that for none of the bridged compounds, a very large increase of fluorescence quantum yields is observed, we can draw the conclusion that the main access to the conical intersection(s) has not been blocked by the substitution pattern employed. According to recent calculations on s3-s [47], one of the most likely bonds to be involved in the CI is bond 2, i.e. the second flexible bond adjacent to the benzthiazole moiety which is unbridged in all the compounds. Thus, experiment and calculations seem to support each other.

4.3. Access to the conical intersection

Several photochemical reactions have been discussed in the context that they might occur on a barrierless potential without involvement of an activation energy. An early example were triphenylmethane dyes like crystal violet, which exhibit a fractional viscosity dependence, i.e. their nonradiative decay rate constant depends on solvent viscosity η according to Eq. (3), where $x=0.66$ [48] or 0.8 [44,49]:

$$k_{nr} = \eta^{-x} \quad (3)$$

This behaviour translates directly to the observed Arrhenius slope E_a which is either equal to that of solvent mobility, $E_{\eta}(x=1)$ or somewhat smaller [44,50].

Various mathematical models have been used to account for these findings, from simple diffusive ones [51] to stochastic kinetic models on parabolic or flat potentials [52,53].

In the case of the kinetics of TICT formation, a similar observation, $E_a < E_{\eta}$ has been made and interpreted as evidence for a barrierless reaction potential [23,54]. This barrierless model was highly controversially discussed in view of an alternative model involving polarity-dependent activation energies [55,56]. Recently, the combination of pressure- and temperature dependent data allowed to show that the barrier along the reaction path is clearly absent [50] and that the observed variation in the reaction rate constants for different compounds therefore derives from differences of the preexponential factor [57].

For the unsymmetric cyanines studied here, we observe a similar relation $E_a \leq E_{\eta}$ which we therefore also interpret as evidence for a barrierless reaction leading to P^* . The reaction rate constant k_{nr} is comparatively slow, only around $2.5 \times 10^9 \text{ s}^{-1}$ at room temperature for s3-s, slowing down down to $3.1 \times 10^6 \text{ s}^{-1}$ at 146 K. This is much slower than for crystal violet in the same solvent ethanol ($> 2 \times 10^{11} \text{ s}^{-1}$ at room temperature [58]; $1 \times 10^9 \text{ s}^{-1}$ at 146 K. [44]) or for DMABN in low-viscosity solvents ($\geq 1 \times 10^{11} \text{ s}^{-1}$ [59]). Given that all the reactions discussed are barrierless, we have to ascribe the observed differences entirely to the preexponential factor which is strongly reduced for the asymmetric cyanines s3-s, s3-o and s3-c (factor ca. > 100 with respect to crystal violet). We tentatively ascribe this strong reduction to the different shape of the potential leading to the conical intersection and possibly a different number of twisted bonds involved: in the case of crystal violet, sterical hindrance leads to a nonplanar geometry of ground and Franck Condon excited state, and the angular difference to a limiting conformation with 90° twist is strongly reduced. For these “pretwisted” geometries, the stochastic models [52] predict an enhancement of the reaction rate which has been verified in a number of studies using TICT compounds [57,60]. In the case of s3-s and derivatives, which are near-planar in the ground state, the dynamics of the access to the fully twisted conformations will therefore be reduced even without involvement of an activation barrier because the flat barrierless potential region which leads to the conical intersection is wider [53,61].

5. Conclusions

We have shown that the comparison of unbridged and bridged cyanine dyes reveals a broadening of the fluorescence spectra together with some redshift which disappears on cooling. Interestingly, some of the bridged compounds show decreased fluorescence quantum yields as compared to their unbridged counterparts. We have shown that both effects can be explained within a common model involving large-amplitude relaxation to emitting conformations R^* with twisted geometry. The nonradiative decay behaviour is thought to derive from the access to a conical intersection P^* which is reached on a barrierless reaction path from both

the primary excited species E^* and from the relaxed R^* conformations.

Acknowledgements

Support by the Deutsche Forschungsgemeinschaft within projects Re 387/8-1, 8-2 and 436 UKR 113/34 as well as by the Fonds der Chemischen Industrie is gratefully acknowledged.

References

- [1] S. Dähne, D. Leupold, *Angew. Chem.* 78 (1966) 1029.
- [2] S. Dähne, *Science* 199 (1978) 1163.
- [3] S. Dähne, K. Hoffmann, in: W.R. Taft (Ed.), *Progress in Physical Organic Chemistry*, vol. 18, Wiley, New York, 1990.
- [4] A.I. Kiprianov, *Zh. Vsesoyuzn. Khim. Obschestva. im. D.I. Mendeleeva* 7(3) (1962) 317.
- [5] A.I. Kiprianov, G.G. Dyadyusha, F.A. Mikhailenko, *Usp. Khimii* 35 (1966) 823.
- [6] P. Czerney, G. Graneß, E. Birckner, F. Vollmer, W. Rettig, *J. Photochem. Photobiol. A* 89 (1995) 31.
- [7] R.P. Haugland, *Handbook of Fluorescent Probes and Research Chemicals*, Molecular Probes, Eugene, OR, 1996.
- [8] P. Fromherz, K.H. Dambacher, H. Ephardt, A. Lambacher, C.O. Müller, R. Neigl, H. Schaden, O. Schenk, T. Vetter, *Ber. Bunsenges. Phys. Chem.* 45 (1991) 1333.
- [9] M. Blanchard-Desce, R. Wortmann, S. Lebus, J.-M. Lehn, P. Krämer, *Chem. Phys. Lett.* 245 (1995) 526.
- [10] C.B. Gorman, S.R. Marder, *Proc. Natl. Acad. Sci. USA* 90 (1993) 11297.
- [11] C. Rulliere, *Chem. Phys. Lett.* 43 (1976) 303.
- [12] F. Momicchioli, I. Baraldi, G. Berthier, *Chem. Phys.* 123 (1988) 103.
- [13] M. Caselli, F. Momicchioli, G. Ponterini, *Chem. Phys. Lett.* 216 (1993) 41.
- [14] I. Baraldi, A. Carnevali, F. Momicchioli, G. Ponterini, G. Berthier, *Gazzetta Chim. Italiana* 126 (1996) 211.
- [15] A.S. Tatikolov, N.A. Derevyanko, A.A. Ishchenko, I. Baraldi, M. Caselli, F. Momicchioli, G. Ponterini, *Ber. Bunsenges. Phys. Chem.* 99 (1995) 763.
- [16] F. Momicchioli, I. Baraldi, G. Berthier, *Chem. Phys.* 123 (1988) 103.
- [17] M. Dekhtyar, W. Rettig, V. Rozenbaum, *J. Photochem. Photobiol. A Chem.* 120 (1999) 75.
- [18] G. Hielig, W. Lüttke, *Chem. Ber.* 121 (1988) 407.
- [19] S.A. Soper, Q.L. Mattingly, *J. Am. Chem. Soc.* 116 (1994) 3744.
- [20] A.I. Tolmachev, Yu.L. Slominskii, A.A. Ishchenko, in: *Near infrared dyes for high technology applications*, in: S. Daehne, U. Resch-Genger, O.S. Wolfbeis (Eds.), *NATO ASI Series*, 3. High Technology, vol. 52, Kluwer Academic Publishers, Dordrecht, 1998, p. 384.
- [21] Z.R. Grabowski, K. Rotkiewicz, A. Siemiarczuk, D.J. Cowley, W. Baumann, *Nouv. J. Chim.* 3 (1979) 443.
- [22] W. Rettig, *Angew. Chem. Int. Ed. Engl.* 25 (1986) 971.
- [23] E. Lippert, W. Rettig, V. Bonacic-Koutecky, F. Heisel, J.A. Miehé, *Adv. Chem. Phys.* 1 (1987) 68.
- [24] W. Rettig, in: J. Mattay (Ed.), *Topics in Current Chemistry*, vol. 169, Springer, Berlin, 1994, p. 253.
- [25] P. Fromherz, A. Heilemann, *J. Phys. Chem.* 96 (1992) 6964.
- [26] H. Ephardt, P. Fromherz, *J. Phys. Chem.* 98 (1993) 4540.
- [27] C. Röcker, A. Heilemann, P. Fromherz, *J. Phys. Chem.* 100 (1996) 12172.
- [28] B. Strehmel, W. Rettig, *J. Biomedical Optics* 1 (1996) 98.
- [29] B. Strehmel, H. Seifert, W. Rettig, *J. Phys. Chem.* 101 (1997) 2232.

- [30] G.N. Lewis, M. Calvin, *Chem. Rev.* 25 (1939) 273.
- [31] L.J.E. Hofer, R.J. Grabenstetter, E.O. Wiig, *J. Am. Chem. Soc.* 72 (1950) 203.
- [32] R. Lapouyade, K. Czeschka, W. Majenz, W. Rettig, E. Gilibert, C. Rullière, *J. Phys. Chem.* 96 (1992) 9643.
- [33] J.-M. Viallet, F. Dupuy, R. Lapouyade, C. Rulliere, *Chem. Phys. Lett.* 222 (1994) 571.
- [34] E. Abraham, J. Oberle, G. Jonusauskas, R. Lapouyade, K. Minoshima, C. Rulliere, *Chem. Phys.* 219 (1997) 73.
- [35] J. Michl, *Pure Appl. Chem.* 41 (1975) 507.
- [36] J. Michl, V. Bonacic-Koutecký, *Electronic Aspects of Organic Photochemistry*, Wiley, New York, 1990.
- [37] F. Bernardi, M. Olivucci, M.A. Robb, *J. Photochem. Photobiol. A* 105 (1997) 365.
- [38] W. Rettig, J. Majenz, *Chem. Phys. Lett.* 154 (1989) 335.
- [39] W. Rettig, W. Majenz, R. Lapouyade, G. Haucke, *J. Photochem. Photobiol. A* 62 (1992) 415.
- [40] L. Brooker, F. White, G. Keyes, C. Smith, P. Oesper, *J. Am. Chem. Soc.* 63 (1941) 3192.
- [41] A.I. Tolmachev, Yu.L. Slominskii, A.I. Kiprianov, *Dokl. AN SSSR, Ser. Khim.* 177 (1967) 869.
- [42] A.I. Tolmachev, Yu.L. Slominskii, M.A. Kudinova, *Usp. Nauchn. Fotogr.* 22 (1984) 12.
- [43] Y. Hishiki, Patent of Japan no. 7040180 (1970); *C.A.* (1971) 74, 113270j.
- [44] W. Rettig, M. Vogel, *Ber. Bunsenges. Phys. Chem.* 91 (1987) 1241.
- [45] M. Garavelli, T. Vreven, P. Celani, F. Bernardi, M.A. Robb, M. Olivucci, *J. Am. Chem. Soc.* 120 (1998) 1285.
- [46] M. Garavelli, P. Celani, F. Bernardi, M.A. Robb, M. Olivucci, *J. Am. Chem. Soc.* 119 (1997) 6891.
- [47] M. Dekhtyar, M. Sczepan, W. Rettig, in preparation.
- [48] T. Förster, G. Hoffmann, *Z. Phys. Chem. N.F.* 75 (1971) 63.
- [49] M. Vogel, W. Rettig, *Ber. Bunsenges. Phys. Chem.* 89 (1985) 962.
- [50] W. Rettig, R. Fritz, D. Braun, *J. Phys. Chem. A* 101 (1997) 6830.
- [51] G. Oster, Y. Nishijima, *J. Am. Chem. Soc.* 78 (1956) 1581.
- [52] B. Bagchi, G.R. Fleming, D.W. Oxtoby, *J. Chem. Phys.* 78 (1983) 7375.
- [53] B. Bagchi, G.R. Fleming, *J. Phys. Chem.* 94 (1990) 9.
- [54] F. Heisel, J.A. Miehe, J.M.G. Martinho, *Chem. Phys.* 98 (1985) 243.
- [55] J.M. Hicks, M.T. Vandersall, Z. Babarogic, K.B. Eisenthal, *Chem. Phys. Lett.* 116 (1985) 18.
- [56] J.M. Hicks, M.T. Vandersall, E.V. Sitzmann, K.B. Eisenthal, *Chem. Phys. Lett.* 135 (1987) 413.
- [57] W. Rettig, R. Gleiter, *J. Phys. Chem.* 89 (1985) 4676.
- [58] D. Ben-Amotz, C.B. Harris, *Chem. Phys. Lett.* 119 (1985) 305.
- [59] P. Changenet, P. Plaza, M.M. Martin, Y.H. Meyer, *J. Phys. Chem. A* 101 (1997) 8186.
- [60] W. Rettig, *Ber. Bunsenges. Phys. Chem.* 95 (1991) 259.
- [61] D. Braun, W. Rettig, *Chem. Phys. Lett.* 268 (1997) 110.